Virology 529 (2019) 101–110

Contents lists available at ScienceDirect

Virology

journal homepage: www.elsevier.com/locate/virology

Avian H5N1 influenza virus infection causes severe pneumonia in the Northern tree shrew (*Tupaia belangeri*)

Takahiro Sanada[a], Fumihiko Yasui[a,*], Tomoko Honda[a], Mohammad Enamul Hoque Kayesh[b], Jun-ichiro Takano[c], Yumiko Shiogama[c], Yasuhiro Yasutomi[c], Kyoko Tsukiyama-Kohara[b], Michinori Kohara[a,*]

[a] Department of Microbiology and Cell Biology, Tokyo Metropolitan Institute of Medical Science, 2-1-6, Kamikitazawa, Setagaya-ku, Tokyo 156-8506, Japan
[b] Transboundary Animal Diseases Centre, Joint Faculty of Veterinary Medicine, Kagoshima University, 1-21-24, Korimoto, Kagoshima-city, Kagoshima 890-0065, Japan
[c] Laboratory of Immunoregulation and Vaccine Research, Tsukuba Primate Research Center, National Institute of Biomedical Innovation, Health and Nutrition, 1-1 Hachimandai, Tsukuba, Ibaraki 305-0843, Japan

ARTICLE INFO

Keywords:
Avian influenza virus
H5N1
H7N9
Tree shrew
Tupaia belangeri

ABSTRACT

Avian-origin influenza viruses like H5N1 and H7N9 often cause severe symptoms with high mortality in humans. Animal models are useful for clarification of the mechanisms of pathogenicity of these infections. In this study, to expand the potential utility of the Northern tree shrew (*Tupaia belangeri*) for influenza virus infection, we assessed the pathogenicity of H5N1 and H7N9 avian influenza viruses in tupaia. Infectious virus was detected continuously from nasal, oral, tracheal, and conjunctival swab samples in the animals infected with these viruses. H5N1 influenza virus infection of tupaia caused severe diffuse pneumonia with fever and weight loss. In contrast, H7N9 influenza virus infection caused focal pneumonia. The severity of pneumonia was correlated with proinflammatory cytokine transcript levels. These results indicated that tupaia can be another suitable animal model for avian influenza virus research.

1. Introduction

Avian influenza viruses frequently are not transmitted between humans but may occasionally infect humans through direct or indirect contact. To date, a total of 860 cases of human infection with H5N1 influenza virus, including 454 deaths, have been reported from 16 countries (World Health Organization, 2018). In H7N9 influenza virus infection, a total of 1567 human cases, including at least 615 deaths, have been reported (World Health Organization, 2018).

Although human infection with avian influenza virus can yield a range of symptoms, clinical features of these infections in human include high fever with cough and severe pneumonia (Bui et al., 2016). Because of the high mortality compared with seasonal influenza virus infection, human infection with avian-origin influenza virus is a major world-wide public health concern (Bui et al., 2016).

Until recently, ferrets and nonhuman primates have been the most appropriate animal models for human influenza virus research (Bouvier, 2015). Ferrets are susceptible to a wide variety of human influenza virus strains without prior adaptation, and symptoms of influenza virus infection in ferrets are similar to those in humans (Belser et al., 2011). Also, ferrets have been used as an important tool for modelling of influenza virus transmission (Bouvier, 2015). Nonhuman primates such as macaques are also susceptible to human influenza virus isolates and show human-like illness (Shichinohe et al., 2016). However, because of high investigation costs, including specific caging and facility requirements, and due to relatively lower commercial availability, only a limited number of researchers can use ferrets and nonhuman primates for this purpose.

The Northern tree shrew (*Tupaia belangeri*), which belongs to the family Tupaiidae, is a small mammal, squirrel-like in appearance, that has a body weight of about 100–150 g (Tsukiyama-Kohara and Kohara, 2014). One of the appealing features of tupaia is the species' genetic closeness to human (Fan et al., 2013). Thus, tupaia has been used in a variety of research fields (Hai-Ying et al., 2016; Lee et al., 2016). In infectious disease research, tupaia has been shown to be susceptible to human-pathogenic viruses such as hepatitis B virus (HBV) and hepatitis C virus (HCV), leading to the use of this species primarily in research on hepatitis viruses (Amako et al., 2010; Sanada et al., 2016; Walter et al., 1996). In addition, Yang et al. (2013) demonstrated that tupaia is susceptible to H1N1 influenza virus infection, with the animal showing

* Corresponding authors.
E-mail addresses: yasui-fm@igakuken.or.jp (F. Yasui), kohara-mc@igakuken.or.jp (M. Kohara).

https://doi.org/10.1016/j.virol.2019.01.015
Received 6 September 2018; Received in revised form 14 January 2019; Accepted 14 January 2019
Available online 19 January 2019

mild respiratory symptoms following exposure.

In the present study, we tested the potential utility of the tupaia animal model for influenza virus infection by infecting the animals with H5N1 and H7N9 influenza viruses and assessing the pathogenicity of these viruses.

2. Materials and methods

2.1. Ethics statement

This study was carried out in strict accordance with the *Guidelines for Animal Experimentation of the Japanese Association for Laboratory Animal Science* and the recommendations in the *Guide for the Care and Use of Laboratory Animals* of the National Institutes of Health. All protocols were approved by the Tokyo Metropolitan Institute of Medical Science Animal Experimental Committee (Permission no.: 17066).

2.2. Viruses

H5N1 highly pathogenic avian influenza virus (HPAIV) A/Vietnam/UT3040/2004, isolated from a human patient in Vietnam (Le et al., 2010), was kindly provided by Dr. Yoshihiro Kawaoka (University of Tokyo, Japan). H7N9 low pathogenic avian influenza virus (LPAIV) A/Anhui/1/2013, isolated from a human patient in China (Gao et al., 2013; Watanabe et al., 2013), was kindly provided by Dr. Takato Odagiri (National Institute of Infectious Diseases, Japan). Viruses were propagated in Madin-Darby canine kidney (MDCK) cells as previously described (Yasui et al., 2016).

2.3. Animals

Northern tree shrews (*T. belangeri*) were purchased from the Kunming Institute of Zoology, Chinese Academy of Sciences. Tupaias were bred in animal facilities of Kagoshima University and Tsukuba Primate Research Center for experimental use. Twelve healthy adult (six-month- to four-year-old) tupaias were used in this study. All animals were confirmed seronegative to H5N1 and H7N9 influenza viruses by enzyme-linked immunosorbent assay (ELISA) before use in the experiment. At least 2 weeks before virus infection, a telemetry probe (TA11ETA-F10; Data Sciences International, New Brighton, MN, United States) was implanted in the abdominal cavity of each animal to monitor body temperature and locomotor activity. Body temperature was recorded for 10 s every 10 min. Locomotor activity was recorded continuously, and the sum of activity counts, from the entire previous 10 min, was reported in arbitrary units (a.u.). Activity counts were recorded when the animal moved in three dimensions, with the number of counts generated depending on both distance and speed of movement.

All animal experiments were carried out at a biosafety level-3 animal facility of the Tokyo Metropolitan Institute of Medical Science.

2.4. Virus infection

We studied three tupaia groups (n = 4 per group; H5N1, H7N9, and Mock). Tupaias were inoculated with a per-animal total of 1.0×10^6 plaque-forming units (PFU) of virus diluted in vehicle (minimum essential medium (MEM) containing 0.1% bovine serum albumin (BSA), 100 U/mL penicillin G, and 100 μg/mL streptomycin). Viruses were inoculated into the nostrils (50 μL per nostril) and trachea (100 μL) by aerosolized administration (IA-1C-R and FMJ-250; Penn-Century, Wyndmoor, PA, United States), and onto the tonsils (15 μL per tonsil) and conjunctivae (10 μL per eye) with pipette. An equivalent volume of vehicle was inoculated to each tupaia of the Mock group. Tupaias were observed daily. Under anesthesia induced by intramuscular injection of ketamine (50 mg/kg) and subcutaneous injection of atropine (0.33 mg/kg), their body weights were measured, and swab samples were collected daily. Swab samples were collected from nasal cavities, conjunctivae, oral cavity, and trachea using cotton sticks, and the sticks were then dipped into 1 mL of MEM containing 0.1% BSA. Sera were collected at − 2 and 7 days post-infection (dpi). All animals were euthanized at 7 dpi, and internal organs were collected, weighed, and used for further experiments.

2.5. Titration of influenza virus

Viral titers in swab samples were determined by $TCID_{50}$ assay as described previously (Nakayama et al., 2013). The $TCID_{50}$ of each swab sample was calculated by the Behrens-Karber method. The detection limit of the virus titer assay was 0.75 $\log_{10}TCID_{50}$/mL.

2.6. Histopathological analysis

Tissue sections from each lobe of lung from each tupaia at 7 dpi were fixed with 10% neutral buffered formalin solution (Wako Pure Chemical Industries, Osaka, Japan) and embedded in paraffin. The samples then were sectioned at 4-μm thicknesses, transferred to slides, and stained with hematoxylin and eosin (H&E). Histological changes were evaluated as described previously (Yasui et al., 2016). For each lung lobe section, 15 randomly selected microscopic fields were captured through a 20× objective lens using a microscope (BZ-X710; Keyence, Osaka, Japan). Each field was graded visually on a scale from 0 to 7, defined as follows: 0, normal lung; 1, mild destruction of epithelium in trachea and bronchus; 2, mild infiltration of inflammatory cells around the periphery of bronchiole; 3, moderate infiltration of inflammatory cells around the alveolar walls, resulting in alveolar thickening; 4, mild alveolar injury accompanied by vascular damage (< 10%); 5, moderate alveolar and vascular injury (10–30%); 6, severe alveolar injury with hyaline membrane-accompanied alveolar hemorrhage (< 50%); and 7, severe alveolar injury with hyaline membrane and alveolar hemorrhage (≥ 50%). The mean value of the grades obtained for all fields was used as the grade of visual lung injury.

2.7. Viral RNA quantification

Tissue samples were homogenized using a BioMasher II (Nippi, Tokyo, Japan) in nine volumes of Leibovitz's L-15 medium (Thermo Fisher Scientific, Waltham, MA, United States). Total RNA samples were extracted from the homogenates using QIAamp Viral RNA Mini kits (Qiagen, Hilden, Germany) according to the manufacturer's instructions. Viral RNA was quantified by quantitative reverse transcription polymerase chain reaction (qRT-PCR), as previously described (Sakurai et al., 2011).

2.8. In situ hybridization analysis

Digoxigenin (DIG) -labeled RNA probes against positive- and negative-strand RNAs for the gene encoding the nucleoprotein (NP) of A/Anhui/1/2013 (H7N9) were prepared as described in our previous study (Ogiwara et al., 2014). The DIG-labeled RNA probes for the gene encoding the NP of H5N1 virus consisted of reagents that had been prepared in the previous study (Ogiwara et al., 2014); these probes were used for detecting the positive- and negative-strand RNAs of A/Vietnam/UT3040/2004 (H5N1). Briefly, formalin-fixed lung tissue samples were embedded in paraffin, sectioned at 6-μm thicknesses, and mounted on slides. After treatment with 30 μg/mL proteinase K for 30 min at 37 °C, the tissue slides were vigorously washed with diethyl pyrocarbonate-treated phosphate-buffered saline (PBS). RNA probes (at 200 ng/mL) were used for hybridizing to the NP-encoding RNAs of these avian influenza viruses. To detect DIG-labeled probe, the tissue slides were incubated with an alkaline phosphatase-labeled sheep anti-DIG antibody (Roche, Basel, Switzerland), and the color was developed with the 5-bromo-4-chloro-3-indolyl phosphate/nitro blue tetrazolium

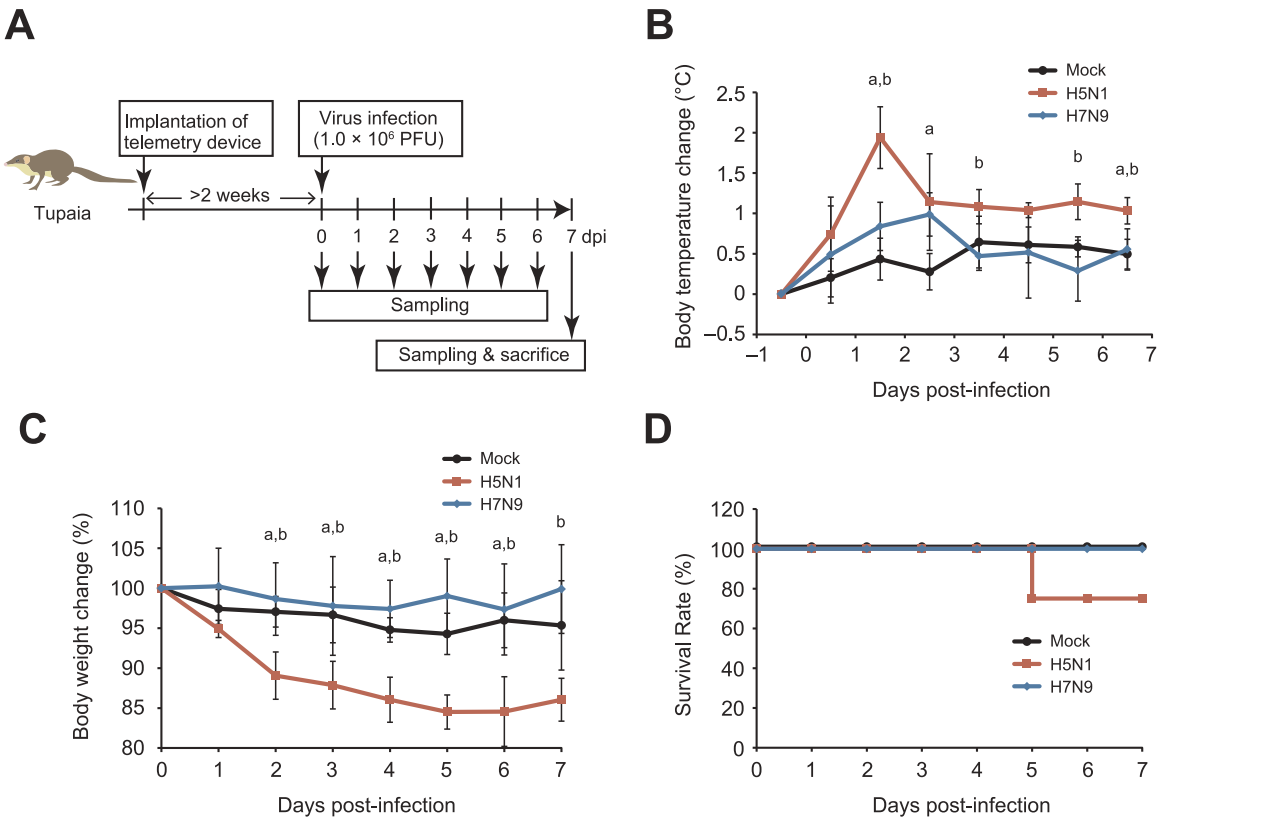

Fig. 1. Clinical symptoms in tupaia after infection with avian influenza viruses. (A) Experimental schedule of influenza virus infection in tupaia. (B) Body temperature changes of tupaias infected with influenza virus. Average temperatures of each tupaia from 9 p.m. to 7 a.m. every night were calculated from temperatures recorded every 10 min. Values at the nominal day − 0.5 were calculated as the average of those from 9 p.m. on day − 1 to 7 a.m. on day 0 before infection; values on the nominal day 0.5 were calculated as the average of those from 9 p.m. on day 0–7 a.m. on day 1 after infection; and similar calculations were used to define values for subsequent intervals. (C) Body weight changes of tupaias infected with influenza virus. (D) Survival curve of tupaias infected with influenza virus. For panels (B) and (C), data are from 4 animals per group, except in the H5N1-infected group at 6 and 7 days post-infection (dpi), when the group size was 3 animal due to death of one H5N1-infected animal at 5 dpi. For panel (D), data are from 4 animals per group. For panels (B) and (C), values are shown as mean ± SD. "a" indicates significant differences between Mock and H5N1 groups on a given day, and "b" indicates significant differences between H5N1 and H7N9 groups on a given day, as assessed by the Tukey-Kramer method ($p < 0.05$).

(BCIP/NBT) system. Stained sections were observed using an A2 upright microscope (Carl Zeiss Microimaging, Oberkochen, Germany).

2.9. Detection of antibody responses by ELISA

ELISA plates were prepared by coating with 50 mM carbonate buffer containing 2 μg/mL formaldehyde-inactivated H5N1 or H7N9 virus. The plates were blocked with 200 μL per well of blocking buffer (PBS containing 1% BSA, 0.5% Tween 20, and 2.5 mM EDTA). Next, individual serum samples, diluted 1:100 in blocking buffer, were dispensed into the plates at 50 μL per well. After overnight incubation at 4 °C, the plates were washed three times with PBS containing 0.05% Tween 20 (PBST). Then, the plates were incubated at 37 °C for 1 h with 50 μL/well anti-tupaia-IgG rabbit IgG (raised in-house), diluted to 1 μg/mL in blocking buffer. After the plates were washed three times with PBST, 50 μL/well of peroxidase-conjugated anti-rabbit-IgG antibodies (GE Healthcare, Chicago, IL, United States), diluted 1:10,000 in blocking buffer, were added to the plates. After 1 h of incubation at 37 °C, the plates were washed six times with PBST. Then, 100 μL *o*-phenylenediamine substrate in hydrogen peroxide were added to each well, and the plates were incubated at room temperature for 30 min. The reaction was stopped by the addition of 50 μL/well of 2 M sulfuric acid. The absorbance was measured at 492 nm, and the values of pre-infection (− 2 dpi) samples were subtracted from the values of the respective post-infection (7 dpi) samples to obtain the optical density (OD) value of each individual sample.

2.10. Hemagglutination inhibition (HI) assay

HI assays were performed according to the modified method of the previous study (Yasui et al., 2016). Briefly, serum samples were heat-inactivated at 56 °C for 30 min and then subjected to 2-fold serial dilutions with PBS. Two-fold serial dilutions of 25 μL of the inactivated sera in U-bottom microplates were incubated for 1 h at room temperature with 25 μL of 4 hemagglutination units of A/Vietnam/UT3040/2004 (H5N1) or A/Anhui/1/2013 (H7N9). Then, 50 μL 0.75% chicken red blood cells (Kohjin Bio, Saitama, Japan) were added to each well. HI titers were determined after incubation for 30 min at room temperature as the reciprocal of the maximum dilution of serum that completely inhibited hemagglutination. Since the starting dilution of serum was 1:10, the detection limit was 10.

2.11. Plaque reduction neutralization (PRNT) assay

Serum samples were heat-inactivated at 56 °C for 30 min and then subjected to 4-fold serial dilutions. Four-fold serial dilutions of the inactivated sera were incubated with 50 PFU of A/Vietnam/UT3040/2004 (H5N1) or A/Anhui/1/2013 (H7N9) for 1 h at 37 °C. Each mixture (100 μL) was used to inoculate one well of a 6-well plated seeded with MDCK cells; the plates then were incubated for an additional hour at 37 °C. After washing with MEM containing 0.11% sodium bicarbonate and 2 mM L-glutamine, the MDCK cells were overlaid (2 mL/well) with 0.8% agarose in MEM supplemented with 1% BSA, 2 mM L-glutamine,

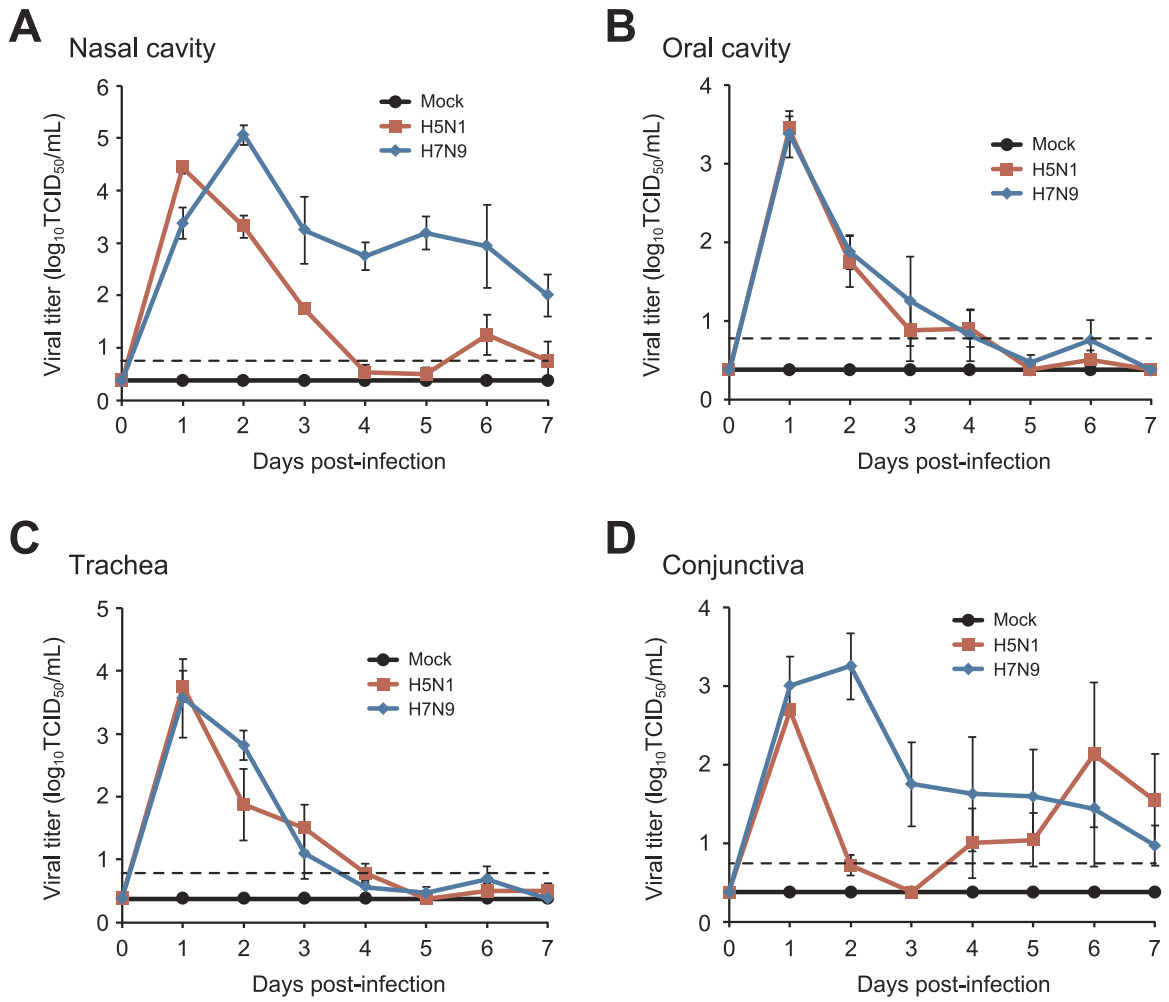

Fig. 2. Temporal changes of viral titer in swab samples. Viral titer in nasal (A), oral (B), tracheal (C), and conjunctival (D) swab samples collected from tupaias infected with influenza virus. Horizontal broken lines indicate the detection limit (0.75 $\log_{10}$TCID$_{50}$/mL). Viral titers below the detection limit are plotted as 0.375. Data are from 4 animals per group, except in the H5N1-infected group at 6 and 7 days post-infection (dpi), when group size was 3 animals due to death of one H5N1-infected animal at 5 dpi. Values are shown as geometric mean ± SD.

vitamins, and 10 μg/mL acetylated trypsin. After 3 days incubation at 37 °C, the cells were fixed with 10% neutral buffered formalin solution. The neutralizing antibody titer of each serum sample was determined as the reciprocal of the maximum dilution of the serum that reduced the number of plaques by 50% or more as compared to wells infected with virus in the absence of serum.

2.12. Measurement of cytokine transcript level

Total RNA was extracted from a lung segment (right lower lobe) of each animal using an RNeasy Mini kit (Qiagen) according to the manufacturer's protocol.

Quantification of each cytokine-encoding mRNA was performed by qRT-PCR using Brilliant III Ultra-Fast SYBR Green QRT-PCR Master Mix (Agilent Technologies, Santa Clara, CA, United States) as previously described (Kayesh et al., 2017). The mRNA expression levels of genes encoding tupaia interferon gamma (*IFNG*), interleukin-6 (*IL6*), and tumor necrosis factor alpha (*TNFA*) were measured, and the mRNA expression levels of tupaia genes encoding glyceraldehyde-3-phosphate dehydrogenase (*GAPDH*) and beta-actin (*ACTB*) were measured as endogenous controls. Thermal cycling conditions were as follows: reverse transcription by incubation at 50 °C for 10 min; initial denaturation by incubation at 95 °C for 3 min; and amplification by 40 cycles of incubation at 95 °C for 5 s and 60 °C (*IFNG*, *IL6*, and *GAPDH*) or 65 °C (*TNFA* and *ACTB*) for 10 s. Primers used to detect the *IFNG* transcript were as follows: forward primer (5′-TACACTGGCTTTCCTGCTTTCT ATC-3′) and reverse primer (5′-TTTTGTCACTCTCCTCTGTCCAA-3′). Other primers used for the cytokine transcript level measurement were as described previously (Kayesh et al., 2017).

2.13. Statistical analyses

Statistical analyses were performed with R software version 3.2.5 (https://www.r-project.org/). Student's *t*-test and the Tukey-Kramer test (two-tailed) were used to conduct statistical analyses of the data. *p* values lower than 0.05 were considered significant.

3. Results

3.1. H5N1 influenza virus infection causes clinical symptoms in tupaia

To evaluate the pathogenicity of H5N1 and H7N9 influenza viruses in tupaia, animals were inoculated with either A/Vietnam/UT3040/2004 (H5N1) or A/Anhui/1/2013 (H7N9) virus (total 1.0×10^6 PFU/250 μL) into their nostrils (50 μL per nostril) and trachea (100 μL) by aerosolized administration, and onto the tonsils (15 μL per tonsil) and conjunctivae (10 μL per eye) by pipette (Fig. 1A). A/Vietnam/UT3040/2004 is a H5N1 HPAIV isolated from a human patient in Vietnam (Le et al., 2010); A/Anhui/1/2013 is a H7N9 LPAIV isolated from a human patient in China (Gao et al., 2013; Watanabe et al., 2013). After H5N1

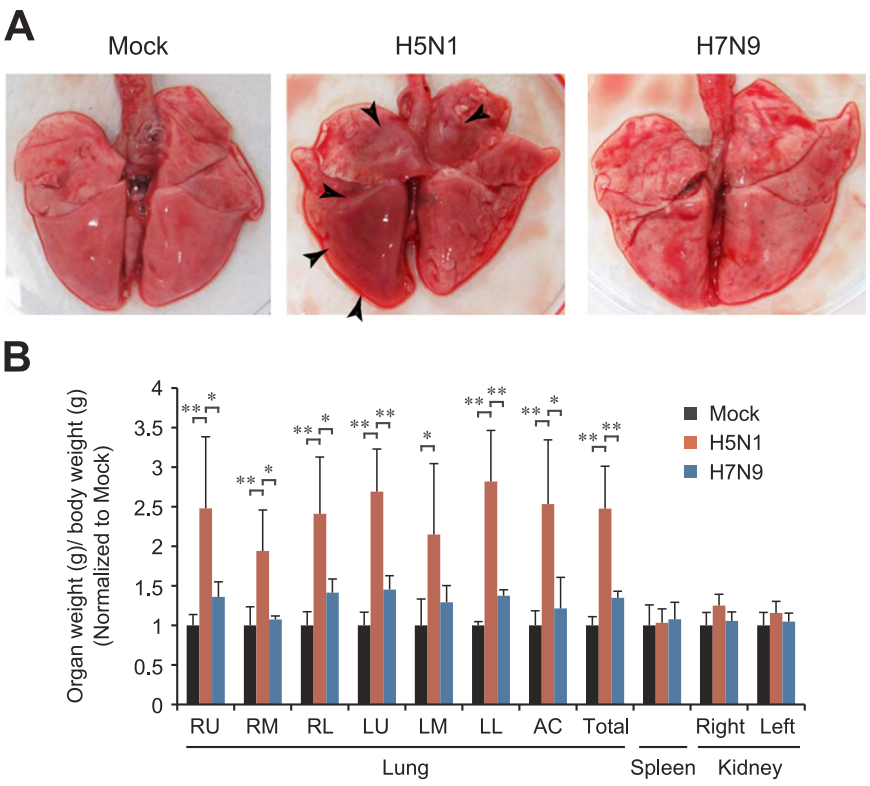

Fig. 3. Gross pathological changes of the lungs of tupaia infected with avian influenza viruses. (A) Representative gross appearance of lungs from Mock-, H5N1-, and H7N9- infected tupaia at 7 days post-infection. H5N1 infection caused visible pneumonia in lung (arrowheads). (B) The ratio of each organ weight from influenza virus-infected tupaia to the respective organ weight from Mock-infected tupaias. Data are from 4 (Mock and H7N9) or 3 (H5N1) animals per group. Values are shown as mean ± SD. Lung lobes: RU, right upper; RM, right middle; RL, right lower; LU, left upper; LM, left middle; LL, left lower; AC, accessory. Significant differences were calculated by the Tukey-Kramer method (*$p < 0.05$, **$p < 0.01$). Where not indicated, differences were not significant ($p > 0.05$).

virus infection, tupaias showed significantly elevated body temperature (Fig. 1B) and body weight loss starting from 2 dpi compared with animals subjected to Mock infection (Fig. 1C). The H5N1-infected animals also exhibited a nominal decline of locomotor activity, although the effect fell short of statistical significance (Supplementary Fig. 1). At 5 dpi, one tupaia (out of four) succumbed to H5N1 virus infection (Fig. 1D). In contrast, H7N9 virus infection caused no significant changes of body weight, body temperature, or locomotor activity compared with Mock infection, and no H7N9-infected animal died before the scheduled sacrifice (Fig. 1B–D and Supplementary Fig. 1).

3.2. Infectious viruses are detected from swab samples of tupaias infected with H5N1 and H7N9 influenza viruses

To evaluate the replication and shedding characteristics of influenza viruses in tupaia, we collected swab samples from the nasal cavity, oral cavity, trachea, and conjunctiva of tupaias infected with either H5N1 or H7N9 influenza virus, and determined the viral titers by $TCID_{50}$ assay. In H5N1-infected animals, viral titers in nasal, oral, and tracheal swabs peaked at 1 dpi (Fig. 2A–C), and then began to decline gradually through 5 dpi, before increasing at 6 dpi. Viral titer in conjunctival swabs also peaked at 1 dpi (Fig. 2D), before subsequently declining to below the limit of detection at 3 dpi. Interestingly, viral titer in conjunctival swabs subsequently increased from 4 dpi, achieving a second peak at 6 dpi. In H7N9-infected animals, viral kinetics in the oral and tracheal swabs were similar to those in H5N1-infected animals, but viral kinetics in nasal and conjunctival swabs were different. Viral titers in these samples peaked at 2 dpi, and then declined to a level that was maintained through 7 dpi. These results indicated that H5N1 and H7N9 influenza viruses propagated in tupaia.

3.3. H5N1 influenza virus infection causes severe pneumonia in tupaia

To reveal whether influenza virus infection in tupaia causes pathological changes, we collected the organs from influenza virus-infected tupaias at 7 dpi, and examined these samples through histopathological analysis.

In gross appearance, lungs from Mock-infected tupaias were pink without abnormalities (left in Fig. 3A). Lungs from H7N9-infected tupaias were similar to those of Mock-infected tupaias (right in Fig. 3A). In contrast, most areas of lungs from H5N1-infected tupaias were dark red, indicating that severe inflammation and congestion had occurred (arrowheads, in the middle of Fig. 3A).

Next, we compared the weight of each organ among the Mock, H5N1, and H7N9 infection groups. It is well known that pneumonia results in increased lung weight (Sidwell et al., 2001). The weights of all lobes of lungs from the H5N1-infected group were significantly heavier than those from the Mock-infected group (Fig. 3B). With the exception of the left middle lobe, the weights of all lung lobes in animals of the H5N1-infected group also were significantly heavier than those from H7N9-infected animals (Fig. 3B). In contrast, there were no significant differences in the lung weights between the Mock- and H7N9-infected groups, nor in the weights of spleen and kidney when comparing the respective organs among the Mock, H5N1, and H7N9 infection groups.

Lung sections were stained with H&E for morphological evaluation. In the lungs from H5N1-infected tupaia, severe acute interstitial pneumonia with diffuse alveolar damage was observed (Fig. 4A and Supplementary Fig. 2). In contrast, histopathological observation of the lungs from tupaia infected with H7N9 influenza virus revealed that inflammation was focal and detected primarily around the bronchioles (Fig. 4A and Supplementary Fig. 2). Consistent with these observations, the histopathological scores in the H5N1-infected tupaia were significantly higher than those in the Mock- and H7N9-infected tupaia (Fig. 4B). In terms of the mean value of the grades obtained for all fields, there was no significant difference in histopathological score between the Mock-infected group and the H7N9-infected group (Fig. 4B). In contrast, the percentage of area with abnormality (histopathological score 2 and more) was significantly higher not only in the H5N1 infection group but also in the H7N9 infection group compared to the Mock infection group (Fig. 4C).

These data indicated that H5N1 virus infection caused severe and extensive pneumonia in tupaia, whereas H7N9 virus infection caused

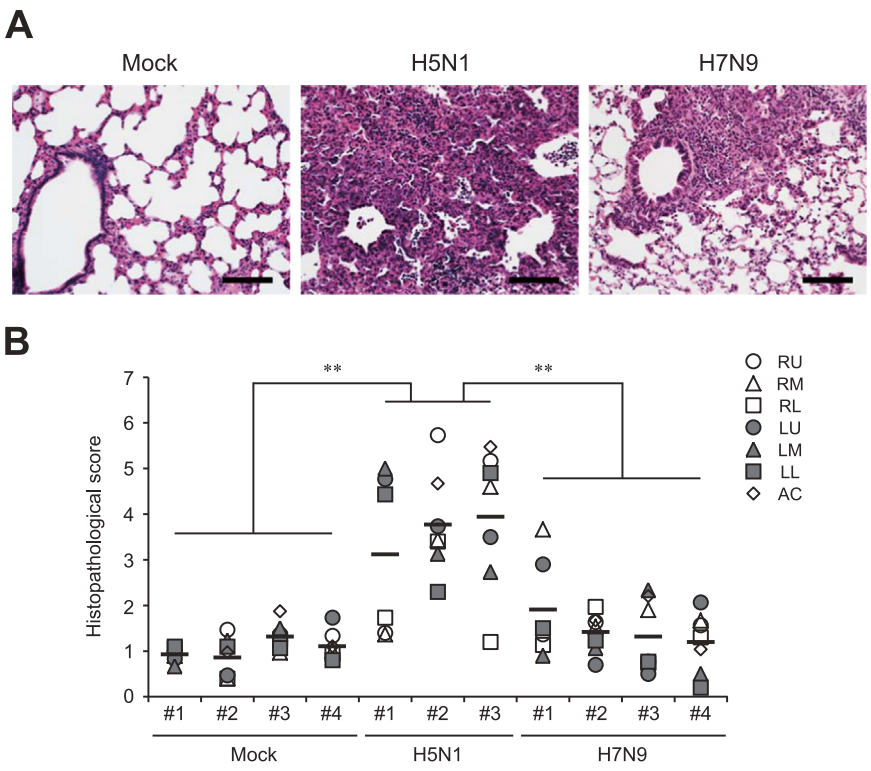

Fig. 4. Histopathological analysis of tupaia lung tissues infected with avian influenza viruses. (A) Representative lung images (hematoxylin and eosin staining) from Mock-, H5N1-, and H7N9- infected tupaia. Bar, 100 μm. (B) Histopathological score of each lung lobe from Mock-, H5N1-, and H7N9-infected tupaia at 7 days post-infection (dpi). Data are from 4 (Mock and H7N9) or 3 (H5N1) individual animals per group. Thick horizontal bars indicate arithmetic mean values for each animal. Lung lobes: RU, right upper; RM, right middle; RL, right lower; LU, left upper; LM, left middle; LL, left lower; AC, accessory. Histological scores were defined as follows: 0, normal lung; 1, mild destruction of epithelium; 2, mild infiltration of inflammatory cells; 3, moderate infiltration of inflammatory cells resulting in alveolar thickening; 4, mild alveolar injury accompanied by vascular damage (< 10%); 5, moderate alveolar and vascular injury (10–30%); 6, severe alveolar injury with hyaline membrane-accompanied alveolar hemorrhage (< 50%); and 7, severe alveolar injury with hyaline membrane and alveolar hemorrhage (≥ 50%). (C) Percentage of area with histopathological score 2 or more in lung from Mock-, H5N1-, and H7N9-infected tupaia at 7 dpi. For (B) and (C), data shown are from 4 (Mock and H7N9) or 3 (H5N1) animals per group. Thick horizontal bars indicate arithmetic mean values in each infection group. Significant differences were calculated by the Tukey-Kramer method (*$p < 0.05$, **$p < 0.01$).

focal pneumonia.

3.4. H5N1 and H7N9 influenza viruses replicate in lung of tupaias

To analyze the association between virus infection and pneumonia, viral RNA levels in the right lower and left lower lobes of lungs at 7 dpi were determined. In the H5N1-infected group, the viral RNA load ranged from 2.8×10^3 to 1.8×10^5 viral RNA copies/mg of tissue (Fig. 5A). In the lungs of the H7N9-infected group, viral RNA was detected from all lower lobes with a single exception. In the animals where viral RNA was detected, the RNA loads ranged from 6.5×10^1 to 3.4×10^4 viral RNA copies/mg of tissue (Fig. 5A). In the lobe that tested negative for viral RNA, the histopathological score was 0.73 and few histopathological changes were observed. In the tupaia that succumbed to H5N1 virus infection at 5 dpi, the right lower lobe harbored a viral RNA load of 5.2×10^7 viral RNA copies/mg of tissue at 5 dpi, a level that exceeded those in the right lower lobes of the animals that survived to 7 dpi.

To investigate whether H5N1 and H7N9 viruses replicate in the lungs of tupaias, in situ hybridization analyses were conducted to detect both positive-strand RNA (messenger RNA, mRNA) and negative-strand RNA (viral RNA, vRNA) for the genes encoding the NP proteins of these viruses. In lung sections of the H5N1 virus-infected tupaia that succumbed at 5 dpi, both the mRNA and vRNA were readily detected in epithelial cells of the bronchial and interstitial regions (Fig. 5B), whereas these RNAs were not readily observed in the lung tissues of H5N1-infected tupaias that survived to 7 dpi. In lung sections of H7N9 virus-infected tupaia, both the mRNA and vRNA were detected in epithelial cells of the alveolar regions from one of the H7N9-infected tupaias at 7 dpi (Fig. 5C). These results indicated that these viruses can infect and replicate in tupaia lung tissues

3.5. H5N1 and H7N9 influenza virus infection induces antibody responses

To investigate the host immune response to influenza virus infection, we used ELISA, HI assay, and PRNT assay to assess the production of antibodies against each influenza virus. IgG antibodies against H5N1 or H7N9 virus were detected at 7 dpi by ELISA (Fig. 6A). By HI assay, antibodies against challenged virus were also detected in all H5N1 virus-infected tupaias (Fig. 6B), but not in H7N9 virus-infected tupaias (Supplementary Fig. 3A). Neutralizing activity (defined as a neutralizing antibody titer ≥ 4) was not detected in any of the serum samples at 7 dpi (Supplementary Fig. 3B).

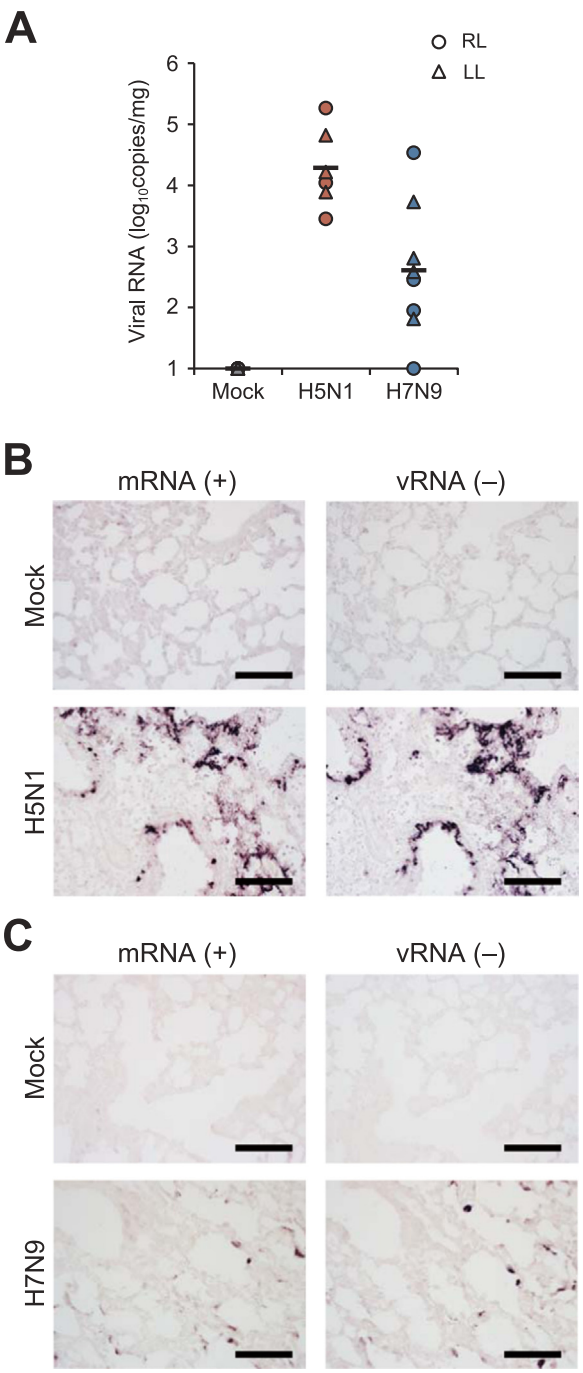

Fig. 5. Detection of influenza virus RNA in lung tissues of tupaias infected with avian influenza viruses. (A) Viral RNA levels in right lower and left lower lobes from Mock-, H5N1-, and H7N9-infected tupaia at 7 days post-infection (dpi). Thick horizontal bars indicate geometric mean values in each infection group. (B) and (C) In situ hybridization analyses of lung tissues of Mock- and H5N1-infected tupaia at 5 dpi (B) or of H7N9-infected tupaia at 7 dpi (C). DIG-labeled RNA probes specific for the positive-strand RNA (messenger RNA, mRNA) and negative-strand RNA (viral RNA, vRNA) for the nucleoprotein (NP)-encoding gene of H5N1 (B) or H7N9 (C) virus were used. Bar, 100 μm.

3.6. Infection with H5N1 virus leads to higher levels of cytokine gene transcripts

Next, to examine inflammatory cytokine responses induced by influenza virus infection, we measured the levels of transcripts of genes encoding proinflammatory cytokines in lung homogenates at 7 dpi. The mean level of tupaia *IFNG* transcript in the lungs of tupaia infected with H5N1 virus was significantly higher than that of Mock-infected tupaias (Fig. 6C). The expression levels of the *IL6* and *TNFA* genes in the H5N1 virus infection group were nominally, but not significantly, elevated compared to those in the Mock infection group (*IL6*: $p = 0.058$, *TNFA*: $p = 0.077$). There was a positive correlation between the viral RNA level and the mRNA level of each cytokine gene. Lung samples from the H5N1-infected animals that showed the highest viral RNA levels also showed the highest levels of *IFNG* and *IL6* transcripts (Table 1). In H7N9 virus-infected animals, the levels of the *IFNG* and *TNFA* transcripts again were nominally, but not significantly, increased compared to those in the Mock infection animals. Lung samples from the H7N9 virus-infected tupaia that showed the highest viral RNA levels also yielded the highest levels of *IFNG*, *IL6*, and *TNFA* transcripts (Table 1). These results indicated that stronger cytokine gene expression responses were induced in the H5N1 virus infection group than in the Mock and H7N9 virus infection groups, an observation that was consistent with the findings of the histopathological study.

4. Discussion

In the present study, we demonstrated that infection of tupaia with two different serotypes of avian influenza viruses causes pneumonia. Infectious viruses were continuously detected in the nasal cavity, oral cavity, trachea, and conjunctiva, and viral RNA also was detected from the lungs of H5N1- and H7N9-infected tupaias at 7 dpi. The symptoms in tupaia were similar to those observed in human. The severity of pneumonia correlated with the expression levels of transcripts encoding proinflammatory cytokines. Our serological analysis showed that viral infection induced the development of influenza virus-specific antibodies in tupaia. Notably, the two viral strains used in the present study had not been adapted to tupaia before use in this investigation. The similarity of symptoms between tupaias and humans might reflect the genetic proximity of these species. Tupaias are genetically closer to primates than are other non-primate mammals, including rodents (Fan et al., 2013), which may engender the similarity of influenza virus pathogenicity in tupaia and human. One effect of this genetic proximity may be the shared distribution of sialic acid receptors, which are known to serve as influenza virus receptors. Distribution of sialic acid receptors strongly associates with host specificity, viral tropism, and pathogenicity (Stevens et al., 2006). It has been reported that the α2,6 sialic acid receptors (which serve as human influenza virus receptors) are distributed primarily in the trachea and bronchus of tupaia, and α2,3 sialic acid receptors (which serve as avian influenza virus receptors) are distributed primarily in the bronchiole and alveolus of tupaia (Yang et al., 2013). This distribution pattern is similar to that in human (Shinya et al., 2006). In human, avian influenza viruses are known to infect the lower respiratory tract, resulting in pneumonia (Nicholls et al., 2007); the same region may have been infected in tupaia in the present study. These data indicated that tupaia has potential utility as an animal model for the analysis of the pathogenicity of influenza viruses, and for the evaluation of the efficacy of vaccines and antiviral drugs.

Among the established animal models of human influenza, ferret is thought to be the animal model that most accurately mimics human influenza virus infection. Similar to human cases, ferrets infected with H5N1 or H7N9 show clinical signs and symptoms, including fever, sneezing, weight loss, nasal discharge, and death (Govorkova et al., 2005; Watanabe et al., 2013). Airborne transmission in ferret has been used to assess the pandemic potential of emerging influenza viruses in humans. Furthermore, recent study has demonstrated that inoculation of the viruses at low doses by aerosol exposure route leads to productive infection in ferrets (Gustin et al., 2011). In tupaia, severe symptoms including pneumonia, fever, weight loss, and death were observed following H5N1 infection, and relatively mild symptoms were observed following H7N9 infection; in both cases, the symptoms were quite similar to those reported for the respective virus serotypes used for

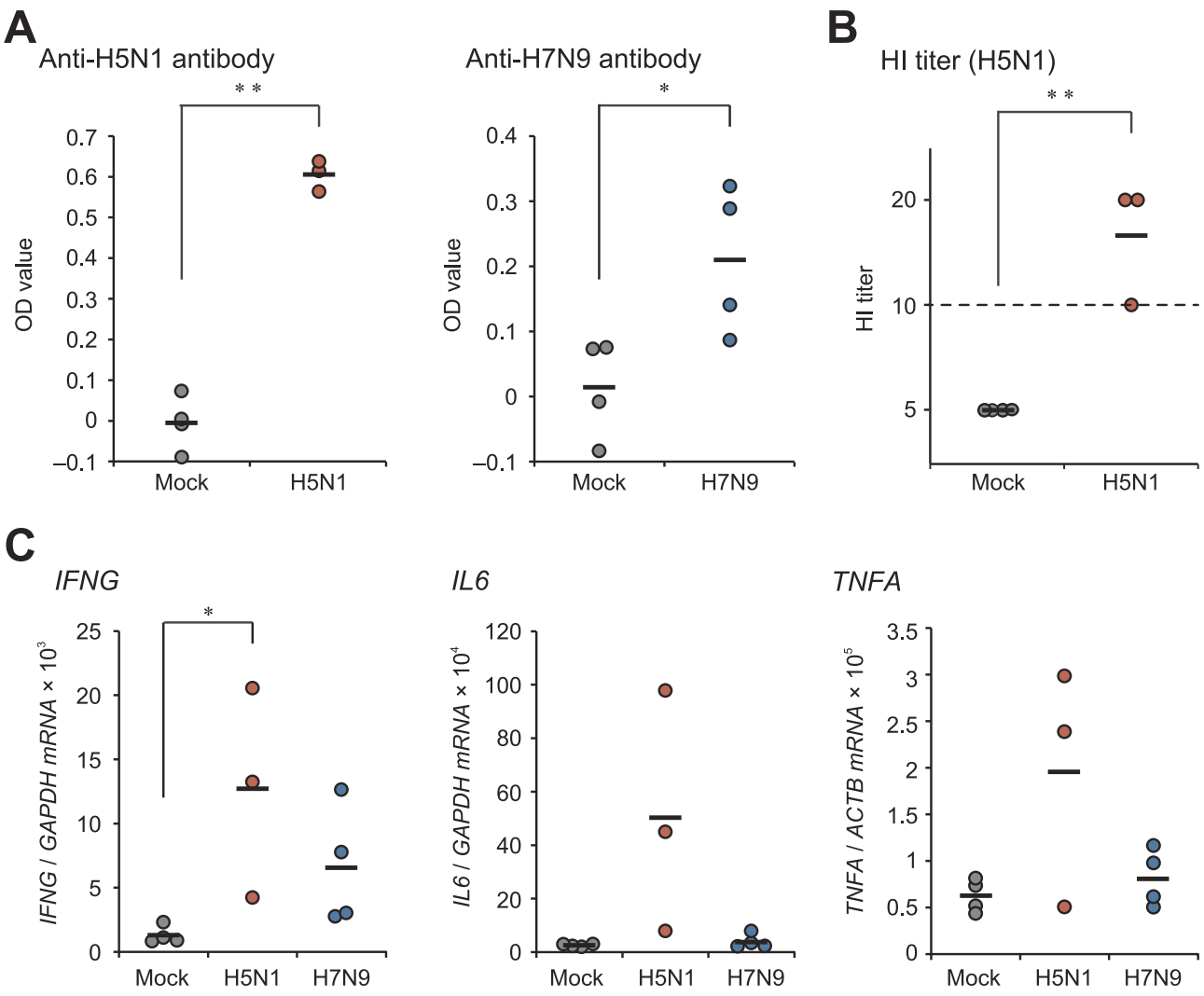

Fig. 6. Host immune responses of tupaia against avian influenza virus infection. (A) IgG response (as determined by enzyme-linked immunosorbent assay (ELISA)) to H5N1 virus (left) and H7N9 virus (right) in tupaias infected by either H5N1 or H7N9 virus. The values of pre-infection (− 2 days post-infection (dpi)) samples were subtracted from the values of the corresponding post-infection (7 dpi) samples to obtain the optical density (OD) value of each individual sample. The mean ± SD of background values (− 2 dpi) of anti-H5N1 antibody detection ELISA and anti-H7N9 antibody detection ELISA were 0.62 ± 0.05 and 0.61 ± 0.08, respectively. (B) Hemagglutination inhibition (HI) titer to H5N1 virus in tupaias infected by H5N1 at 7 dpi. Horizontal broken lines indicate the detection limit (HI titer, 10). HI titers below the detection limit are plotted as 5. (C) The gene expression levels in the lung of Mock-, H5N1-, and H7N9-infected tupaia at 7 dpi. The transcript levels were normalized against those of tupaia *GAPDH* (*IFNG* and *IL6*) or *ACTB* (*TNFA*). Data are from 4 (Mock and H7N9) or 3 (H5N1) individual animals per group. For panels (A) and (C), thick horizontal bars indicate arithmetic mean values in each group. For panel (B), thick horizontal bars indicate geometric mean values in each group. For panels (A) and (B), asterisks indicate significant differences calculated by the Student's *t*-test. For panel (C), asterisks indicate significant differences calculated by the Tukey-Kramer method (*$p < 0.05$, **$p < 0.01$). Where not indicated, differences were not significant ($p > 0.05$).

Table 1
Viral RNA level and cytokine transcript level in right lower lobe from each tupaia.

		Viral RNA (copies/mg)	*IFNG/GAPDH* (× 10^3)	*IL6/GAPDH* (× 10^4)	*TNFA/ACTB* (× 10^5)
Mock	#1	ND	0.82	2.29	0.74
	#2	ND	2.32	1.95	0.52
	#3	ND	0.90	2.91	0.81
	#4	ND	1.11	3.02	0.44
H5N1	#1	2.8E + 03	4.23	7.93	0.51
	#2	1.1E + 04	13.25	45.02	2.98
	#3	1.8E + 05	20.55	97.81	2.39
H7N9	#1	2.8E + 02	2.76	2.14	0.50
	#2	3.4E + 04	12.64	7.89	1.16
	#3	ND	3.02	2.27	0.62
	#4	8.9E + 01	7.77	3.42	0.98

ND, not detected.

infections in ferrets (Govorkova et al., 2005; Watanabe et al., 2013). On the contrary, in the present study, sneezing could not be observed in tupaia model. In addition, airborne transmission has yet not been analyzed in tupaia model. Additionally, here tupaias were infected with viruses through multiple routes according to the previous studies using cynomolgus macaques (Baskin et al., 2009; Brown et al., 2010; de Wit et al., 2014), and the effect of route and amount of exposure on infectivity and pathogenesis remains to be investigated. The number of animals used in the present study was limited; future studies incorporating larger numbers of animals are expected to provide more insight into the pathogenesis and transmissibility of influenza in the tupaia model.

Following H7N9 virus infection in tupaia, virus was continuously detected in nasal samples during the experimental period (through 7 dpi). In a previous study, H7N9 virus infected and replicated efficiently in the upper and lower respiratory tracts in human (Chan et al., 2013; van Riel et al., 2013) and macaque (de Wit et al., 2014; Shichinohe

et al., 2016). In tupaia, H7N9 may infect and replicate efficiently in the upper respiratory tract, resulting in the persistence of virus secretion in nasal fluid. Given that prolonged virus secretion increases the risk of virus transmission, further studies of H7N9 virus maintenance in the upper respiratory tract will be essential for evaluating the risk of transmission. Interestingly, the tested influenza viruses were continuously in conjunctival swabs following infection with H5N1 and H7N9 viruses. In addition, the kinetics of the H5N1 viral load showed a double-peaked pattern, suggesting that this virus propagates in tupaia conjunctiva. This observation is reminiscent of a previous *ex vivo* analysis that showed that avian influenza viruses (H5N1 and H7N9) infect and replicate in human conjunctival epithelial cells (Chan et al., 2010). Thus, avian-origin influenza virus infection via the conjunctiva might occur in humans. Using the tupaia model, we expect to be able to evaluate the risk of infection via the conjunctiva by assessing the replication ability of the virus in this animal model.

There were significant differences in symptoms between H5N1 infection and H7N9 infection in tupaia. H5N1 infection in tupaia caused severe diffuse pneumonia with fever and weight loss. In contrast, H7N9 infection in tupaia caused focal pneumonia without changes in body temperature or weight, even though the level of secreted virus in H7N9-infected tupaia was similar to that in H5N1-infected animals. The difference in host cytokine response in tupaia correlated with the difference in pathogenicity between H5N1 and H7N9 influenza virus. In human infection, the pathogenicity of influenza virus infection is known to be strongly associated with cytokine response (Guo and Thomas, 2017). This difference in pathogenicity between H5N1 and H7N9 virus infection in tupaia may be associated with the difference in epidemiologic characteristics between H5N1 and H7N9 virus infection. The median age of human cases with H5N1 is approximately 20 years (Qin et al., 2015), and the case fatality rate is higher in younger age groups (Abdel-Ghafar et al., 2008). In contrast, in human cases of H7N9 infection, the median age is approximately 60 years (Qin et al., 2015), and the case fatality rate is higher in older age groups (Skowronski et al., 2013). The tupaias used in the present study were relatively young; thus, H5N1 infection might have caused more severe symptoms than did H7N9 in this study. In addition, fatality in cases of H7N9 infection tends to be associated with underlying disease (Gong et al., 2014). Various factors would affect the severity of H7N9 infection. Further studies, including examinations of H7N9 infection in older tupaia, are expected to elucidate the mechanism of high mortality in humans infected with avian influenza virus.

While tupaia has the advantage of genetic proximity to human, several further issues will need to be addressed to establish tupaia as a laboratory animal model. Research tools such as antibodies against tupaia molecules and PCR systems to evaluate gene expression levels are under construction, but are not sufficiently advanced at the present time. Recently, the whole-genome sequence of tupaia was published (Fan et al., 2013). This large genetic resource is expected to accelerate the development of research tools for tupaia. In addition, construction of transgenic tupaia using spermatogonial stem cells has been reported (Li et al., 2017). We postulate that the development of a gene editing method will be critical for use of this species as a standard laboratory animal. The advantages of tupaia are easier handling and lower cost of breeding compared to ferret and nonhuman primate. Tupaia could serve as an alternative animal model not only for influenza virus infection but also for various other areas of biomedical research.

In conclusion, we examined the pathogenicity of H5N1 and H7N9 influenza virus infection in tupaia. Notably, H5N1 infection caused severe and extensive pneumonia with fever and weight loss. More severe symptoms correlated with the stronger induction of expression of genes encoding proinflammatory cytokines. We propose that tupaia would be a suitable animal model for avian influenza virus research.

Acknowledgments

We express our gratitude to the following individuals: Dr. Yoshihiro Kawaoka of the Institute of Medical Science, University of Tokyo, for providing the A/Vietnam/UT3040/2004 (H5N1) isolate; Dr. Takato Odagiri of the National Institute of Infectious Diseases for providing the A/Anhui/1/2013 (H7N9) isolate; and Dr. Naoki Yamamoto for technical assistance with the tupaia experiments.

Financial support

This work was supported by grants from the Ministry of Education, Culture, Sports, Science and Technology (15H04739), and the Tokyo Metropolitan Government, Japan.

Potential conflicts of interest

The authors have declared no conflict of interest.

Appendix A. Supplementary material

Supplementary data associated with this article can be found in the online version at doi:10.1016/j.virol.2019.01.015.

References

Abdel-Ghafar, A.N., Chotpitayasunondh, T., Gao, Z., Hayden, F.G., Nguyen, D.H., de Jong, M.D., Naghdaliyev, A., Peiris, J.S., Shindo, N., Soeroso, S., Uyeki, T.M., 2008. Update on avian influenza A (H5N1) virus infection in humans. N. Engl. J. Med. 358, 261–273.

Amako, Y., Tsukiyama-Kohara, K., Katsume, A., Hirata, Y., Sekiguchi, S., Tobita, Y., Hayashi, Y., Hishima, T., Funata, N., Yonekawa, H., Kohara, M., 2010. Pathogenesis of hepatitis C virus infection in Tupaia belangeri. J. Virol. 84, 303–311.

Baskin, C.R., Bielefeldt-Ohmann, H., Tumpey, T.M., Sabourin, P.J., Long, J.P., Garcia-Sastre, A., Tolnay, A.E., Albrecht, R., Pyles, J.A., Olson, P.H., Aicher, L.D., Rosenzweig, E.R., Murali-Krishna, K., Clark, E.A., Kotur, M.S., Fornek, J.L., Proll, S., Palermo, R.E., Sabourin, C.L., Katze, M.G., 2009. Early and sustained innate immune response defines pathology and death in nonhuman primates infected by highly pathogenic influenza virus. Proc. Natl. Acad. Sci. USA 106, 3455–3460.

Belser, J.A., Katz, J.M., Tumpey, T.M., 2011. The ferret as a model organism to study influenza A virus infection. Dis. Model. Mech. 4, 575–579.

Bouvier, N.M., 2015. Animal models for influenza virus transmission studies: a historical perspective. Curr. Opin. Virol. 13, 101–108.

Brown, J.N., Palermo, R.E., Baskin, C.R., Gritsenko, M., Sabourin, P.J., Long, J.P., Sabourin, C.L., Bielefeldt-Ohmann, H., Garcia-Sastre, A., Albrecht, R., Tumpey, T.M., Jacobs, J.M., Smith, R.D., Katze, M.G., 2010. Macaque proteome response to highly pathogenic avian influenza and 1918 reassortant influenza virus infections. J. Virol. 84, 12058–12068.

Bui, C., Bethmont, A., Chughtai, A.A., Gardner, L., Sarkar, S., Hassan, S., Seale, H., MacIntyre, C.R., 2016. A systematic review of the comparative epidemiology of avian and human influenza A H5N1 and H7N9 – lessons and unanswered questions. Transbound. Emerg. Dis. 63, 602–620.

Chan, M.C., Chan, R.W., Chan, L.L., Mok, C.K., Hui, K.P., Fong, J.H., Tao, K.P., Poon, L.L., Nicholls, J.M., Guan, Y., Peiris, J.S., 2013. Tropism and innate host responses of a novel avian influenza A H7N9 virus: an analysis of ex-vivo and in-vitro cultures of the human respiratory tract. Lancet Respir. Med. 1, 534–542.

Chan, M.C., Chan, R.W., Yu, W.C., Ho, C.C., Yuen, K.M., Fong, J.H., Tang, L.L., Lai, W.W., Lo, A.C., Chui, W.H., Sihoe, A.D., Kwong, D.L., Wong, D.S., Tsao, G.S., Poon, L.L., Guan, Y., Nicholls, J.M., Peiris, J.S., 2010. Tropism and innate host responses of the 2009 pandemic H1N1 influenza virus in ex vivo and in vitro cultures of human conjunctiva and respiratory tract. Am. J. Pathol. 176, 1828–1840.

de Wit, E., Rasmussen, A.L., Feldmann, F., Bushmaker, T., Martellaro, C., Haddock, E., Okumura, A., Proll, S.C., Chang, J., Gardner, D., Katze, M.G., Munster, V.J., Feldmann, H., 2014. Influenza virus A/Anhui/1/2013 (H7N9) replicates efficiently in the upper and lower respiratory tracts of cynomolgus macaques. MBio 5.

Fan, Y., Huang, Z.Y., Cao, C.C., Chen, C.S., Chen, Y.X., Fan, D.D., He, J., Hou, H.L., Hu, L., Hu, X.T., Jiang, X.T., Lai, R., Lang, Y.S., Liang, B., Liao, S.G., Mu, D., Ma, Y.Y., Niu, Y.Y., Sun, X.Q., Xia, J.Q., Xiao, J., Xiong, Z.Q., Xu, L., Yang, L., Zhang, Y., Zhao, W., Zhao, X.D., Zheng, Y.T., Zhou, J.M., Zhu, Y.B., Zhang, G.J., Wang, J., Yao, Y.G., 2013. Genome of the Chinese tree shrew. Nat. Commun. 4, 1426.

Gao, R., Cao, B., Hu, Y., Feng, Z., Wang, D., Hu, W., Chen, J., Jie, Z., Qiu, H., Xu, K., Xu, X., Lu, H., Zhu, W., Gao, Z., Xiang, N., Shen, Y., He, Z., Gu, Y., Zhang, Z., Yang, Y., Zhao, X., Zhou, L., Li, X., Zou, S., Zhang, Y., Yang, L., Guo, J., Dong, J., Li, Q., Dong, L., Zhu, Y., Bai, T., Wang, S., Hao, P., Yang, W., Han, J., Yu, H., Li, D., Gao, G.F., Wu, G., Wang, Y., Yuan, Z., Shu, Y., 2013. Human infection with a novel avian-origin influenza A (H7N9) virus. N. Engl. J. Med. 368, 1888–1897.

Gong, Z., Lv, H., Ding, H., Han, J., Sun, J., Chai, C., Cai, J., Yu, Z., Chen, E., 2014. Epidemiology of the avian influenza A (H7N9) outbreak in Zhejiang Province, China.

BMC Infect. Dis. 14, 244.
Govorkova, E.A., Rehg, J.E., Krauss, S., Yen, H.L., Guan, Y., Peiris, M., Nguyen, T.D., Hanh, T.H., Puthavathana, P., Long, H.T., Buranathai, C., Lim, W., Webster, R.G., Hoffmann, E., 2005. Lethality to ferrets of H5N1 influenza viruses isolated from humans and poultry in 2004. J. Virol. 79, 2191–2198.
Guo, X.J., Thomas, P.G., 2017. New fronts emerge in the influenza cytokine storm. Semin. Immunopathol. 39, 541–550.
Gustin, K.M., Belser, J.A., Wadford, D.A., Pearce, M.B., Katz, J.M., Tumpey, T.M., Maines, T.R., 2011. Influenza virus aerosol exposure and analytical system for ferrets. Proc. Natl. Acad. Sci. USA 108, 8432–8437.
Hai-Ying, C., Nagano, K., Ezzikouri, S., Yamaguchi, C., Kayesh, M.E., Rebbani, K., Kitab, B., Nakano, H., Kouji, H., Kohara, M., Tsukiyama-Kohara, K., 2016. Establishment of an intermittent cold stress model using Tupaia belangeri and evaluation of compound C737 targeting neuron-restrictive silencer factor. Exp. Anim. 65, 285–292.
Kayesh, M.E.H., Ezzikouri, S., Chi, H., Sanada, T., Yamamoto, N., Kitab, B., Haraguchi, T., Matsuyama, R., Nkogue, C.N., Hatai, H., Miyoshi, N., Murakami, S., Tanaka, Y., Takano, J.I., Shiogama, Y., Yasutomi, Y., Kohara, M., Tsukiyama-Kohara, K., 2017. Interferon-beta response is impaired by hepatitis B virus infection in Tupaia belangeri. Virus Res. 237, 47–57.
Le, Q.M., Ito, M., Muramoto, Y., Hoang, P.V., Vuong, C.D., Sakai-Tagawa, Y., Kiso, M., Ozawa, M., Takano, R., Kawaoka, Y., 2010. Pathogenicity of highly pathogenic avian H5N1 influenza A viruses isolated from humans between 2003 and 2008 in northern Vietnam. J. Gen. Virol. 91, 2485–2490.
Lee, K.S., Huang, X., Fitzpatrick, D., 2016. Topology of ON and OFF inputs in visual cortex enables an invariant columnar architecture. Nature 533, 90–94.
Li, C.H., Yan, L.Z., Ban, W.Z., Tu, Q., Wu, Y., Wang, L., Bi, R., Ji, S., Ma, Y.H., Nie, W.H., Lv, L.B., Yao, Y.G., Zhao, X.D., Zheng, P., 2017. Long-term propagation of tree shrew spermatogonial stem cells in culture and successful generation of transgenic offspring. Cell Res. 27, 241–252.
Nakayama, M., Shichinohe, S., Itoh, Y., Ishigaki, H., Kitano, M., Arikata, M., Pham, V.L., Ishida, H., Kitagawa, N., Okamatsu, M., Sakoda, Y., Ichikawa, T., Tsuchiya, H., Nakamura, S., Le, Q.M., Ito, M., Kawaoka, Y., Kida, H., Ogasawara, K., 2013. Protection against H5N1 highly pathogenic avian and pandemic (H1N1) 2009 influenza virus infection in cynomolgus monkeys by an inactivated H5N1 whole particle vaccine. PLoS One 8, e82740.
Nicholls, J.M., Chan, M.C., Chan, W.Y., Wong, H.K., Cheung, C.Y., Kwong, D.L., Wong, M.P., Chui, W.H., Poon, L.L., Tsao, S.W., Guan, Y., Peiris, J.S., 2007. Tropism of avian influenza A (H5N1) in the upper and lower respiratory tract. Nat. Med. 13, 147–149.
Ogiwara, H., Yasui, F., Munekata, K., Takagi-Kamiya, A., Munakata, T., Nomura, N., Shibasaki, F., Kuwahara, K., Sakaguchi, N., Sakoda, Y., Kida, H., Kohara, M., 2014. Histopathological evaluation of the diversity of cells susceptible to H5N1 virulent avian influenza virus. Am. J. Pathol. 184, 171–183.
Qin, Y., Horby, P.W., Tsang, T.K., Chen, E., Gao, L., Ou, J., Nguyen, T.H., Duong, T.N., Gasimov, V., Feng, L., Wu, P., Jiang, H., Ren, X., Peng, Z., Li, S., Li, M., Zheng, J., Liu, S., Hu, S., Hong, R., Farrar, J.J., Leung, G.M., Gao, G.F., Cowling, B.J., Yu, H., 2015. Differences in the epidemiology of human cases of avian influenza A(H7N9) and A(H5N1) viruses infection. Clin. Infect. Dis. 61, 563–571.
Sakurai, A., Nomura, N., Nanba, R., Sinkai, T., Iwaki, T., Obayashi, T., Hashimoto, K., Hasegawa, M., Sakoda, Y., Naito, A., Morizane, Y., Hosaka, M., Tsuboi, K., Kida, H., Kai, A., Shibasaki, F., 2011. Rapid typing of influenza viruses using super high-speed quantitative real-time PCR. J. Virol. Methods 178, 75–81.
Sanada, T., Tsukiyama-Kohara, K., Yamamoto, N., Ezzikouri, S., Benjelloun, S., Murakami, S., Tanaka, Y., Tateno, C., Kohara, M., 2016. Property of hepatitis B virus replication in Tupaia belangeri hepatocytes. Biochem. Biophys. Res. Commun. 469, 229–235.
Shichinohe, S., Itoh, Y., Nakayama, M., Ozaki, H., Soda, K., Ishigaki, H., Okamatsu, M., Sakoda, Y., Kida, H., Ogasawara, K., 2016. Comparison of pathogenicities of H7 avian influenza viruses via intranasal and conjunctival inoculation in cynomolgus macaques. Virology 493, 31–38.
Shinya, K., Ebina, M., Yamada, S., Ono, M., Kasai, N., Kawaoka, Y., 2006. Avian flu: influenza virus receptors in the human airway. Nature 440, 435–436.
Sidwell, R.W., Smee, D.F., Huffman, J.H., Barnard, D.L., Bailey, K.W., Morrey, J.D., Babu, Y.S., 2001. In vivo influenza virus-inhibitory effects of the cyclopentane neuraminidase inhibitor RJW-270201. Antimicrob. Agents Chemother. 45, 749–757.
Skowronski, D.M., Janjua, N.Z., Kwindt, T.L., De Serres, G., 2013. Virus-host interactions and the unusual age and sex distribution of human cases of influenza A(H7N9) in China, April 2013. Eur. Surveill. 18, 20465.
Stevens, J., Blixt, O., Tumpey, T.M., Taubenberger, J.K., Paulson, J.C., Wilson, I.A., 2006. Structure and receptor specificity of the hemagglutinin from an H5N1 influenza virus. Science 312, 404–410.
Tsukiyama-Kohara, K., Kohara, M., 2014. Tupaia belangeri as an experimental animal model for viral infection. Exp. Anim. 63, 367–374.
van Riel, D., Leijten, L.M.E., de Graaf, M., Siegers, J.Y., Short, K.R., Spronken, M.I.J., Schrauwen, E.J.A., Fouchier, R.A.M., Osterhaus, A., Kuiken, T., 2013. Novel avian-origin influenza A (H7N9) virus attaches to epithelium in both upper and lower respiratory tract of humans. Am. J. Pathol. 183, 1137–1143.
Walter, E., Keist, R., Niederost, B., Pult, I., Blum, H.E., 1996. Hepatitis B virus infection of tupaia hepatocytes in vitro and in vivo. Hepatology 24, 1–5.
Watanabe, T., Kiso, M., Fukuyama, S., Nakajima, N., Imai, M., Yamada, S., Murakami, S., Yamayoshi, S., Iwatsuki-Horimoto, K., Sakoda, Y., Takashita, E., McBride, R., Noda, T., Hatta, M., Imai, H., Zhao, D., Kishida, N., Shirakura, M., de Vries, R.P., Shichinohe, S., Okamatsu, M., Tamura, T., Tomita, Y., Fujimoto, N., Goto, K., Katsura, H., Kawakami, E., Ishikawa, I., Watanabe, S., Ito, M., Sakai-Tagawa, Y., Sugita, Y., Uraki, R., Yamaji, R., Eisfeld, A.J., Zhong, G., Fan, S., Ping, J., Maher, E.A., Hanson, A., Uchida, Y., Saito, T., Ozawa, M., Neumann, G., Kida, H., Odagiri, T., Paulson, J.C., Hasegawa, H., Tashiro, M., Kawaoka, Y., 2013. Characterization of H7N9 influenza A viruses isolated from humans. Nature 501, 551–555.
World Health Organization, 2018. Influenza at the Human-Animal Interface (HAI). Summary and Assessment. (3 March–28 May 2018. Available at: ⟨http://www.who.int/influenza/human_animal_interface/HAI_Risk_Assessment/en/⟩, Accessed 28 November 2018).
Yang, Z.F., Zhao, J., Zhu, Y.T., Wang, Y.T., Liu, R., Zhao, S.S., Li, R.F., Yang, C.G., Li, J.Q., Zhong, N.S., 2013. The tree shrew provides a useful alternative model for the study of influenza H1N1 virus. Virol. J. 10, 111.
Yasui, F., Itoh, Y., Ikejiri, A., Kitabatake, M., Sakaguchi, N., Munekata, K., Shichinohe, S., Hayashi, Y., Ishigaki, H., Nakayama, M., Sakoda, Y., Kida, H., Ogasawara, K., Kohara, M., 2016. Sensitization with vaccinia virus encoding H5N1 hemagglutinin restores immune potential against H5N1 influenza virus. Sci. Rep. 6, 37915.